Small-angle neutron scattering study of the temperature-dependent attractive interaction in dense *L*64 copolymer micellar solutions and its relation to kinetic glass transition

Wei-Ren Chen,[1] Sow-Hsin Chen,[1,*] and Francesco Mallamace[1,2]
[1]*Department of Nuclear Engineering, Massachusetts Institute of Technology, Cambridge, Massachusetts 02139-4307*
[2]*Dipartimento di Fisica e Istituto Nazionale per la Fisica della Materia, Universitá di Messina, Messina, Italy*
(Received 16 April 2002; published 16 August 2002)

We made small-angle neutron scattering (SANS) study of a Pluronic *L*64 micellar system in aqueous solution at high polymer concentrations (wt %), $35\% < c < 53\%$, in a temperature range where a kinetic glass transition has been observed by photon correlation spectroscopy and zero shear viscosity measurements. We analyze SANS intensity distributions assuming that the micelles are spherical and interact among themselves by an effective pair potential, consisting of a hard core plus a narrow attractive square well, the depth of which is temperature dependent. The theory is able to account for the intensity distribution quantitatively when the micellar system is in the liquid phase (but qualitatively when the micellar system is in the glass state), giving values of four parameters: the aggregation number of the micelle *N*, the volume fraction occupied by the micelles ϕ, the fractional width of the square well ε, and the effective temperature $T^* = k_B T/u$, where $-u$ is the depth of the square well. Thus, we are able to assign a point in the phase diagram (the T^*-ϕ plane) for each measured micellar liquid and glass state. Comparison with a phase diagram predicted recently by mode coupling theory calculation allows us to identify the existence of the so-called liquid-to-attractive-glass transition line. We also found the evidence of glass-to-glass transition at volume fraction of 0.54 predicted by the mode coupling theory.

DOI: 10.1103/PhysRevE.66.021403 PACS number(s): 82.70.Dd, 61.12.Ex, 61.25.Hq

I. INTRODUCTION

Previously, we reported an observation of a temperature and concentration dependent structural arrest transition, or a kinetic glass transition (KGT) line, distinct from a percolation line [1], in a copolymer micellar system showing many characteristics of a system having a short-range attractive interaction [2]. We showed that at a fixed polymer concentration, as we approach KGT from the low temperature side, the time evolution of the photon correlation function (PCS) measured in a dynamic light scattering experiment exhibits a fast-slow relaxation scenario. The intermediate scattering function (ISF) begins with a short-time Gaussian-like relaxation, soon turning into a logarithmic decay, followed by a plateau region and then a power-law decay, before evolving into a final, slow α relaxation. The fact that there is a logarithmic time decay region preceding the plateau, suggests that the system state is in the vicinity of a cusplike bifurcation singularity of a A_3 type [3], predicted by mode coupling theory (MCT) for a system having two control parameters [4,5]. The phase boundary marking the KGT, predicted by the MCT, for a system with a hard-core plus a short-range (square well) attractive potential shows the existence of two mutually intersecting branches: one originates from the familiar cage effect due to the excluded volume effect coming from the hard core, and the other from cluster formation due to the short-range attractive tail [3,6].

In this paper, based on an extensive analysis of a set of small-angle neutron scattering (SANS) data taken at high polymer concentrations, we give experimental evidence showing the existence of a liquid-to-glass-to-liquid reentrant KGT. Upon raising the temperature at fixed polymer concentrations in a range of weight fractions, $0.35 < c < 0.53$, the KGT phase boundaries obtained from three different experimental techniques agree within the experimental errors. We give an argument based on experimentally determined parameters, obtained from the SANS data analyses, showing the existence of the attractive branch of the KGT predicted by the mode coupling calculations [3,6]. Our observed reentrant phase behavior can be understood as the result of a double crossing of the attractive branch due to the competition between the temperature dependence of $-u$ (depth of the attractive potential well) and the magnitude of $k_B T$ of the system.

Our micellar system is made by dissolving a triblock copolymer *L*64, one member of Pluronic family [7] used extensively in industrial applications, into D_2O at weight fractions less than 0.53. Pluronic is made of polyethylene oxide (PEO) and polypropylene oxide (PPO) with the two PEO chains placed symmetrically on each end of the PPO chain. The chemical formula of *L*64 is $[(PEO)_{13}\text{-}(PPO)_{30}\text{-}(PEO)_{13}]$, having a molecular weight of 2990 Da and is comprised of PPO:PEO weight ratio of 60:40. At low temperatures, both PEO and PPO are hydrophilic, so that *L*64 chain readily dissolves in water existing as a unimer. As temperature rises, due to the less likelihood of hydrogen-bond formation between water and polymer molecules, PPO tends to become less hydrophilic faster than PEO, thus the copolymer acquires surfactant properties and aggregates to form micelles. Since at higher temperatures, water becomes progressively a poor solvent to both PPO and PEO chains, the effective micelle-micelle interaction be-

*Author to whom all correspondence should be addressed. Email address: sowhsin@mit.edu

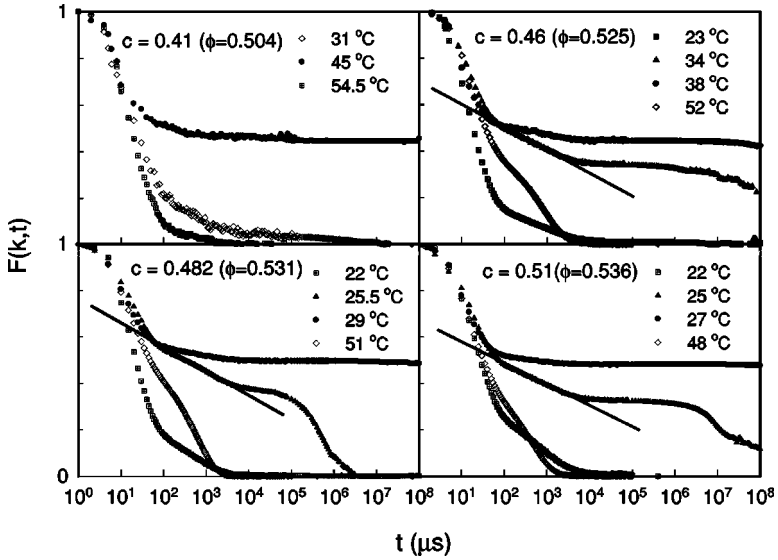

FIG. 1. Typical examples of the intermediate scattering functions $F(k,t)$ as measured by photon correlation spectroscopy (PCS), at different concentrations, as a function of temperature, showing the ergodic-to-nonergodic-to-ergodic transition. In the three panels, we highlight the occurrence of a region of a logarithmic time dependence preceding the plateau region for the system in the ergodic state just before the transition.

comes attractive. At low concentrations, the attraction increases significantly as a function of temperature so that it leads to an existence of a critical point at $c=0.05$ and $T=330.9$ K, as was shown by a series of studies [8,9].

II. EXPERIMENT

The Pluronic L64 triblock copolymer sample was obtained from BASF Inc. After necessary purification procedure to remove hydrophobic impurities, the polymer was dissolved in deuterated water purchased from Cambridge Isotopes Inc. In the three different experiments mentioned above, photon correlation spectroscopy (PCS), zero shear viscosity measurements, and SANS, we have explored the dynamic state and the structure of the system as a function of T at different c (weight fraction of the polymer). Purified $L64$ samples were prepared by using a standard procedure [9]. During the experiments the temperature stability was controlled to within $\pm 0.1\,^{\circ}$C. Viscosity measurements have been made with a strain controlled rheometer, using a double wall Couette geometry. To ensure a linear response, we work at the applied strains $\gamma=0.04$ [10]. PCS measurements were made at a scattering angle $\theta=90\,^{\circ}$, using a continuous wave solid state laser (Verdi-Coherent) operating at 50 mW ($\lambda=5120$ Å) and an optical scattering cell of a diameter 1 cm in a refractive index matching bath. The intensity data were also corrected for turbidity and multiple scattering effects. The PCS data were taken using a digital correlator with a logarithmic sampling time scale. The latter feature allows us to describe accurately both the short-time and the very long-time regions, up to time of the order of seconds. From the measured photon correlation function, we have calculated, by using the same procedure describing in Ref. [1], ISF $F(k,t)$.

SANS measurements were made at $NG7$, 40-m SANS spectrometer in the Center for Neutron Research (NIST), and at SAND station of the Intense Pulse Neutron Source (IPNS) in Argonne National Laboratory. At $NG7$, we used incident monochromatic neutrons of wave length $\lambda=5$ Å with $\Delta\lambda/\lambda=11\%$. Sample to detector distance was fixed at 6 m, covering the magnitude of wave vector transfer (k) range 0.008–0.3 Å^{-1}. IPNS generates high energy spallation neutrons by bombarding a heavy metal target with repetitive pulses of 500 MeV protons. After moderation of these high energy neutrons, one selects a pulse of white neutrons with an effective wave length range from 1.5 Å to 14 Å. At SAND all these neutrons are utilized by encoding their individual time of flight and their scattering angles determined by their detected position at a two-dimensional (2D) area detector. The 2D area detector has an active area of 40 $\times 40$ cm^2 and the sample to detector distance is 2 m. This configuration allows a maximum scattering angle of about 9°. The reliable Q range covered in the measurements were from 0.004 Å^{-1} to 0.6 Å^{-1}. Q-resolution functions of both of these SANS spectrometers are Gaussian and well characterized. It is essential that we apply these resolution broadenings to the theoretical cross section when fitting the intensity data. Sample liquid was contained in a flat quartz cell with 1-mm path length. The measured intensity was corrected for background and empty cell contributions and normalized by a reference scattering intensity of a polymer sample of known cross section.

Before entering into a discussion of the method of measuring the effective potential parameters by SANS data analysis, we shall first show two direct experimental evidences of the KGT, using our photon correlation and viscosity data.

Figure 1 shows some ISF obtained by PCS in a concentration range $0.41<c<0.51$, at different temperatures. As can be seen on increasing the temperature, the system, start-

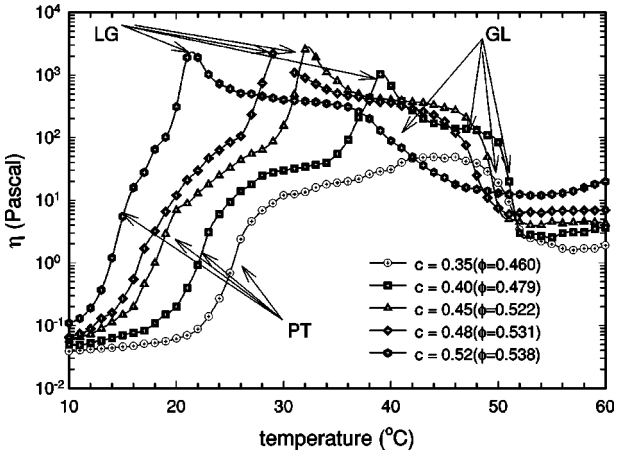

FIG. 2. The zero shear viscosity at five different concentrations as a function of temperature. Starting from low temperatures, the shear viscosity increases steeply, first going through a percolation transition (PT), then a liquid-to-glass (LG) transition, and finally a glass-to-liquid (GL) transition. Note that, for the case of $c=0.35$, there is only the percolation transition.

ing from a liquid state at a lower temperature, where the ISF decays to zero at long time, approaches a KGT characterized by a diverging α relaxation time and the ISF tends to a finite plateau at long time $[F(k,t\rightarrow\infty)=f(k)>0]$. Just before such an ergodic-to-nonergodic transition, the ISF, right after the initial Gaussian-like short-time relaxation, exhibits a time interval with a logarithmic decay (indicated in the figure by a straight line fits) before entering into the plateau region [1]. As discussed above, an important prediction of the MCT calculation for an attractive colloid system is a suggestion that there exists an attractive branch of KGT line near the cusp singularity separating two different glass phases [3,6]. Motivated by this prediction, we extended the study of the

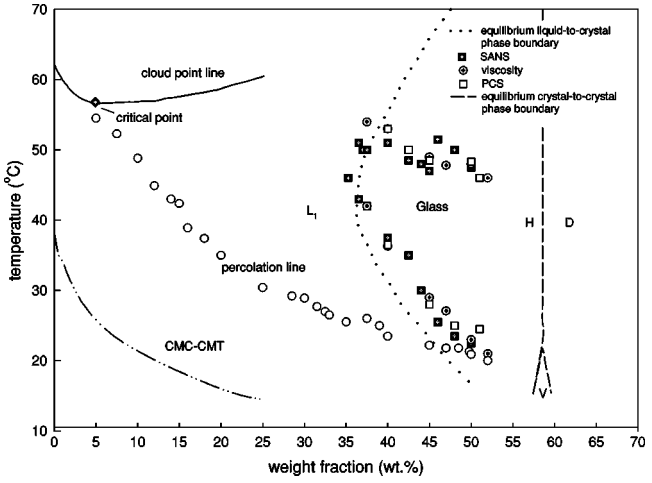

FIG. 3. The phase diagram (in temperature-concentration plane) of Pluronic $L64$ in D_2O solution. The phase diagram contains the CMC-CMT line, cloud point line, percolation line [2], the equilibrium liquid-to-crystal phase boundary (dotted line), the equilibrium crystal-to-crystal phase boundary (dash line) [12], and the reentrant kinetic glass transition (KGT) lines, which are determined by PCS, SANS, and zero shear viscosity measurements, respectively.

micellar system to higher temperatures. Starting from a glass state, upon further increasing the temperature, the measured ISF reveals a surprising reentry from glass-to-liquid state, as seen by the ISF again decaying to zero at higher temperatures.

The low shear viscosity at five different concentrations measured as a function of the temperature is shown in Fig. 2. The viscosity at all concentrations are characterized by an initial increase, starting from viscosity values typical of a liquid ($\eta\sim10^{-2}$ Pa), followed by a flatten-off at the highest temperatures. For the concentration $c=0.35$, the viscosity shows only a single step increase that covers three orders of magnitude. For the remaining concentrations, there is an additional step increase located in a different temperature range. Thus for concentrations $c>0.35$, the overall viscosity increase is about five orders of magnitude. The first step viscosity increase in $L64/D_2O$ micellar system is due to the percolation process that is characteristic of a colloid with a short-range attractive interaction [2]. Figure 3 gives the system phase diagram in which we show the measured percolation points obtained by observation of the power-law frequency dependences of the complex viscosity and elastic and storage components of the shear moduli (G' and G'') as a function of temperature. The second step increase in viscosity in which the viscosity reaches very large absolute values ($>10^3$ Pa), is located in the region of the KGT. We have confirmed it by observing in this temperature range a dramatic modification of shear moduli as the KGT is approached [11]. The elastic component G' becomes larger than the viscous component G'' whereas the frequency dependence of the G' developes a plateau and that of the G'' a minimum. In addition, these frequency dependences can be described in terms of an MCT approach. Finally, the sharp reduction in viscosity and its eventual flatten-off at high temperatures (with final viscosity value of the order of a few pascal, can be related to the reentry of the system into the liquid state.

Figure 3 is the phase diagram of $L64/D_2O$ system in the concentration range $0<c<0.7$. Besides the cloud point curve, its associated critical point and the percolation points, which we have discussed before [2,8,9], we have added the newly found KGT boundaries (symbols) at high concentrations. The dotted line depicts the equilibrium phase boundary between the disordered micellar phase and the ordered liquid crystalline (hexagonal) phase given by Zhang *et al.* [12]. Clearly, the amorphous states in the region of phase space under discussion are metastable states of the system, such as in supercooled liquids. In our system the crystallization would not happen unless the system is disturbed by an applied shear or placed very near to a surface [13]. Thus, it is clear that KGT is observed in a metastable state of the micellar solution, which will last as long as we observe (days).

III. SANS DATA ANALYSIS

The absolute intensity (in unit of cm^{-1}) of neutron scattering from a system of monodispersed micelles can be expressed by the following formula:

$$I(k)=cN\left[\sum_i b_i-\rho_w v_p\right]^2\overline{P}(k)S(k), \tag{1}$$

where c is the concentration of polymer (number of polymers/cm^3), N is the aggregation number of polymers in a micelle, $\Sigma_i b_i$ is the sum of coherent scattering lengths of atoms comprising a polymer molecule, ρ_w is the scattering length density of D_2O, v_p is the molecular volume of the polymer, $\overline{P}(k)$ is the normalized intraparticle structure factor, and $S(k)$ is the intermicellar structure factor.

A. The modified cap-and-gown model for the intraparticle structure factor $\overline{P}(k)$

We assume that the micelle has a compact spherical hydrophorbic core of a radius a, consisting of all the PPO segments with a polymer volume fraction in the core $\phi_p=1$ (i.e., a dry core), and a diffuse corona region consisting of PEO segments and the solvent molecules. The original cap-and-gown model [8] assumes that the radial distribution profile in the corona region is a Gaussian form. However, our analysis of SANS data at high concentrations shows that we need a more diffuse corona region than previously assumed. In this paper, we therefore take the radial profile of the polymer in the corona region to be a power-law decay with the power n to be determined by geometrical constraints. The overall polymer segmental distribution in a micelle can thus be expressed as

$$\phi_p(r)=\begin{cases}1 & \text{for } 0<r<a\\ \left(\dfrac{a}{r}\right)^n & \text{for } r>a.\end{cases} \tag{2}$$

The core radius a and the power n are related by two geometrical constraints. The total volume of the polymer segments in the core is given by the product of the aggregation number N and the PPO segmental volume v_{PPO},

$$\frac{4}{3}\pi a^3=Nv_{\mathrm{PPO}} \quad \text{where } v_{\mathrm{PPO}}=95.4\times 30\ \text{Å}^3. \tag{3}$$

Similarly, the total volume of polymer segments outside the core is given by the product of the aggregation number N and the volume integral of the PEO segmental distribution

$$4\pi\int_a^\infty\left(\frac{a}{r}\right)^n r^2dr=Nv_{\mathrm{PEO}} \quad \text{where } v_{\mathrm{PEO}}=72.4\times 26\ \text{Å}^3. \tag{4}$$

Combining these two constraints, we can write

$$\frac{v_{\mathrm{PPO}}}{v_{\mathrm{PEO}}}=\frac{3\int_a^\infty\left(\frac{a}{r}\right)^n r^2dr}{a^3}=\frac{3}{n-3}=0.658, \tag{5}$$

where 0.658 is the ratio of the known molecular volumes of PPO and PEO segments. From this equation, we obtained a unique value of $n=7.56$.

The particle form factor is then calculated by the following formula:

$$F(k)=\int d^3r(\rho_p-\rho_w)\exp(i\vec{k}\cdot\vec{r})=\frac{4\pi a^2}{k}(\rho_p-\rho_w)\times\left[j_1(ka)+\int_1^\infty\sin(kax)x^{-6.56}dx\right], \tag{6}$$

where $j_1(k)$ is the spherical Bessel function of order one.

It is convenient to define a normalized form factor by dividing $F(k)$ by its value at $k=0$,

$$F(0)=(\rho_p-\rho_w)(V_p^{core}+V_p^{corona})=(\rho_p-\rho_w)\times\frac{4\pi a^3}{3}\left(1+\frac{v_{\mathrm{PEO}}}{v_{\mathrm{PPO}}}\right). \tag{7}$$

Therefore, the normalized form factor is

$$\overline{F}(k)=\frac{F(k)}{F(0)}=\frac{3v_{\mathrm{PPO}}}{v_{\mathrm{PPO}}+v_{\mathrm{PEO}}}\left[\frac{j_1(ka)}{ka}+\int_1^\infty\frac{\sin(kax)}{ka}x^{-6.56}dx\right], \tag{8}$$

which depends on only one parameter, the core radius a. Note that a is tied to the aggregation number N uniquely through Eq. 3. The normalized intraparticle structure factor is then calculated as $\overline{P}(k)=|\overline{F}(k)|^2$.

B. The model for the intermicellar structure factor $S(k)$

A square well potential with a replusive core of diameter R' and the real particle diameter R is used to model a hard sphere with an adhesive surface layer that is introduced to describe the intermicellar attractive interaction. The pairwise potential is defined as

$$V(r)=\begin{cases}+\infty & \text{for } 0<r<R'\\ -u & \text{for } R'<r<R\\ 0 & \text{for } r>R.\end{cases} \tag{9}$$

We define here $\varepsilon=(R-R')/R$ as the fractional well width parameter and $T^*=k_BT/u$ as the effective temperature. Then the intermicellar structure factor is a function of four pameters: the real particle diameter R, the volume fraction ϕ, the fractional well width parameter ε, and the effective temperature T^*. It should be noted that real particle diameter R is tied uniquely to the aggregation number N and the volume fraction ϕ through a relation $\phi=c\pi R^3/6N$.

The Ornstein-Zernike (OZ) equation in Percus-Yevick approximation for this square well potential can be solved analytically to the first order in a series of small ε expansion [14]. The result of the structure factor is given as follows:

$$\frac{1}{S(Q)}-1=24\varphi\left[\alpha f_2(Q)+\beta f_3(Q)+\frac{1}{2}\phi\alpha f_5(Q)\right]+4\phi^2\lambda^2\varepsilon^2\left[f_2(\varepsilon Q)-\frac{1}{2}f_3(\varepsilon Q)\right]+2\phi^2\lambda^2[f_1(Q)-\varepsilon^2 f_1(\varepsilon Q)]-\frac{2\phi\lambda}{\epsilon}\{f_1(Q)-(1-\varepsilon)^2 f_1[(1-\varepsilon)Q]\}-24\phi\{f_2(Q)-(1-\varepsilon)^3 f_2[(1-\varepsilon)Q]\}, \tag{10}$$

where

$$Q=kR,$$

$$\phi=\frac{c\pi R^3}{6N},$$

$$\alpha=\frac{(1+2\phi-\mu)^2}{(1-\phi)^4},$$

$$\beta=-\frac{3\phi(2+\phi)^2-2\mu(1+7\phi+\phi^2)+\mu^2(2+\phi)}{2(1-\phi)^4},$$

$$\mu=\lambda\phi(1-\phi),$$

$$\lambda=\frac{6(\Delta-\sqrt{\Delta^2-\Gamma})}{\phi},$$

$$\Delta=\tau+\frac{\phi}{(1-\phi)}=\frac{1}{12\varepsilon}\exp\left(-\frac{u}{k_BT}\right)+\frac{\phi}{(1-\phi)},$$

$$\Gamma=\frac{\phi(1+\phi/2)}{3(1-\phi)^2},$$

$$f_1(x)=\frac{1-\cos x}{x^2},$$

$$f_2(x)=\frac{\sin x-x\cos x}{x^3},$$

$$f_3(x)=\frac{2x\sin x-(x^2-2)\cos x-2}{x^4},$$

$$f_5(x)=\frac{(4x^3-24x)\sin x-(x^4-12x^2+24)\cos x+24}{x^6}. \tag{11}$$

This formula is accurate in the k region around the first diffraction peak for $\varepsilon<0.05$ [15]. To fit SANS data, the theoretical formula (1) is convoluted with the Gaussian-like resolution function obtained from NIST and IPNS, respectively.

It should be noted that the real volume of a micelle is significantly larger than the volume of N dry polymer chains. It consists of the volume of the N dry polymer chains plus the volumes of the associated hydration water per polymer chain in the corona region. The real volume of the micelle, rather than the polymer volume, determines the thermodynamic quantities such as the osmotic compressibility and the scattering intensities. It further determines the dynamical properties, such as diffusivity and viscosity, of the polymeric micellar solution [14]. Obtaining the real volume of a micelle in a self-consistent way is not a trivial matter. It requires the knowledge of the detailed microstructure such as hydration number per polymer chain. This information on the associated solvent molecules is not available from the theoretical predictions and can be extracted accurately from the analysis of the scattering intensity distributions through the volume fraction ϕ and the aggregation number N.

To summarize the main points of this section, we stress that an absolute SANS intensity distribution can be fitted uniquely with four parameters: the aggregation number N, the volume fraction ϕ, the fractional well width parameter ε, and the effective temperature T^*. The normalized intraparticle structure factor $\overline{P}(k)$ is the function of N only. The intermicellar structure factor $S(k)$ is the function of all the four parameters.

IV. RESULTS AND DISCUSSION

It is our observation that at high enough polymer concentration, SANS intensity distribution from the $L64/D_2O$ micellar system generally consists of a single, sharp interaction peak. A series of SANS intensity distributions taken from the micellar solutions with different polymer concentrations and temperatures have been examined to see whether there is a significant change of the line shape at the ergodic-to-nonergodic-to-ergodic transition temperatures observed by PCS experiment shown in Fig. 1. Part of the results are given in Figs. 4, 5, and 6, respectively. Since there is a single peak in the observed SANS intensity distribution, we can assume that the system is characterized by a single length scale $\Lambda=1/k_{\max}$, where $k_{\max}$ is the peak position of the intensity distribution. It is well known that the absolute intensity in a two-phase system (the micelles and the solvent) is given by a Fourier transform of the Debye correlation function $\Gamma(r)$ and the Debye correlation function in this case must be of the form $\Gamma(r/\Lambda)$. Therefore,

$$I(k)=\langle\eta^2\rangle\int_o^\infty dr\,4\pi r^2 j_o(kr)\Gamma\left(\frac{r}{\Lambda}\right), \tag{12}$$

where $\langle\eta^2\rangle$ is the so-called invariant (not the viscosity).

Now, make a transformation of variables

$$x=\frac{r}{\Lambda}=k_{\max}r,$$

$$y=\frac{k}{k_{\max}} \tag{13}$$

then

$$\frac{k_{\max}^3 I(k)}{\langle \eta^2 \rangle} = \int_o^\infty dx 4\pi x^2 j_o(xy)\Gamma(x). \tag{14}$$

Thus, it can be seen that the scaled intensity $k_{\max}^3 I(k)/\langle \eta^2 \rangle$ is a unique function of $y = k/k_{\max}$. Therefore, if we plot the scaled intensity distributions at different temperatures as a function of y, it would collapse into one single master curve in the liquid state.

The mean particle separation distance that characterizes the unique length scale in the liquid state can best be visualized by the scaling plot. Figure 4 shows a scaling plot of a micellar solution at polymer weight fraction of 35.0 wt % at a series temperatures ranging from 31.0 °C to 59.0 °C. The scaled line shape can be very well approximated by a Lorentzian and the plot of the half width of the Lorentzian line versus temperature is given in the inset. It can be seen that all the scaled intensity distributions are temperature independent and they indeed collapse into one single master curve. According to our latest measurement, this temperature-independent scaled plot is observed for every polymer solution for which the polymer weight fraction is between 25.0 wt % and 35.25 wt %. Figure 4 also indicates that the system is in the liquid state by the fact that all the scaled peaks are considerably broader than the resolution function of the instrument. As we go above the concentration 35.25 wt %, the situation changes dramatically. As an example, we show a scaling plot of a micellar solution with

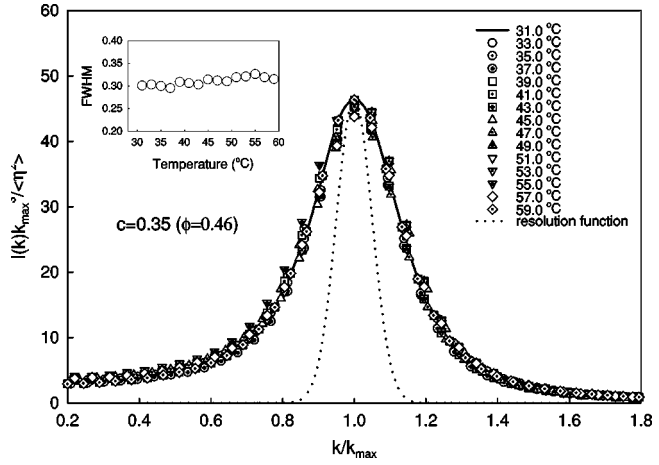

FIG. 4. The scaling plot of SANS intensity distributions of the micellar solution at 35.0 wt % polymer concentration and at different temperatures. It is seen from the figure that the system is indeed characterized by a unique temperature-dependent length scale. Therefore, all the scaled intensities collapse into a single master curve when plotted as a function of $k/k_{\max}$ (with a dimensionless peak height of about 50). The dotted line is the resolution function of the instrument. The fact that the scaling peak (essentially the first diffraction peak of the intermicellar structure factor), is considerably broader than the resolution function indicates that the system is in the liquid state. The inset shows the plot of the dimensionless full width at half maximum (FWHM = 0.30) of all the scaled SANS intensity distributions as a function of temperature.

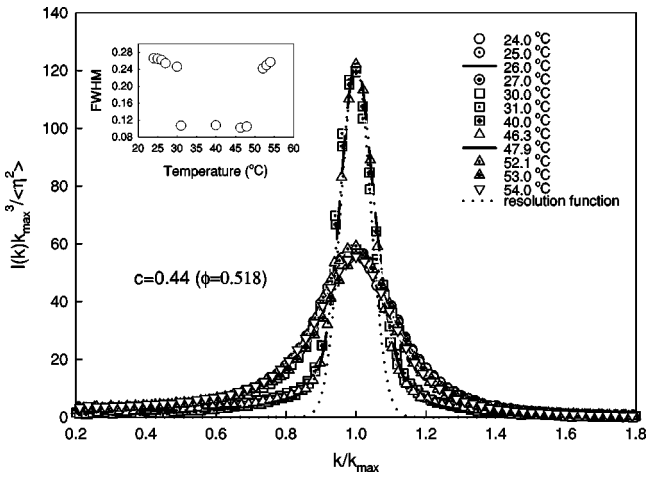

FIG. 5. The scaling plot of SANS intensity distributions of a micellar solution at 44.0 wt % polymer concentration and at different temperatures. It is seen clearly that although the system is still characterized by a temperature-dependent length scale, but there is a temperature-dependent disorder in addition. While the narrower peak is resolution limited, the broader peak is similar to the one observed in the previous figure. If we identify the broader peak to represent the liquid state (with the dimensionless peak height of about 55 and width of 0.26), then the narrower peak should represent the glassy state (an amorphous solid state with the dimensionless peak height of about 120 and width of 0.12). The inset shows the dimensionless FWHM as a function of temperature. It is seen from this plot that the system shows a reentrant liquid-to-glass-to-liquid transition phenomenon, the liquid state below 30 °C and again above 48 °C. The FWHM makes a transition between a value 0.10 and 0.28.

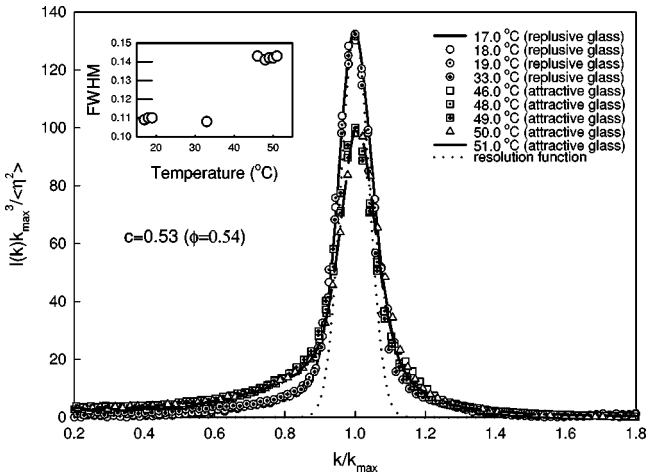

FIG. 6. The scaling plot of SANS intensity distributions of a micellar solution at 53.0 wt % ($\phi = 0.54$) polymer concentration and at different temperatures. It is seen that the system is again characterized by a temperature-dependent length scale. While the narrower peak is resolution limited (with the dimensionless peak height of about 130), the slightly broader peak is also nearly resolution limited (with the dimensionless peak height of about 100). It can be interpreted as showing a glass-to-glass transition (transition between two amorphous solid states with different degrees of disorder). The inset shows the transition of one amorphous state with a dimensionless FWHM of 0.11 to another one with a FWHM of 0.14 at a temperature of 45 °C.

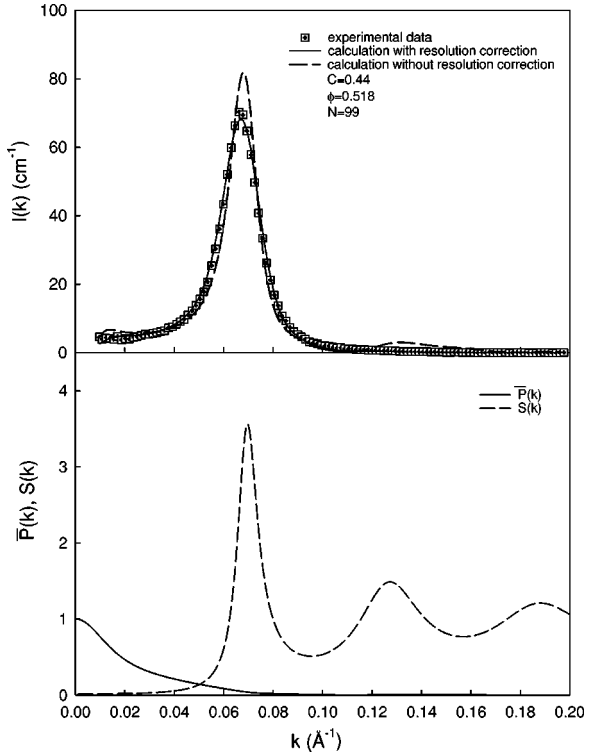

FIG. 7. The upper panel shows the SANS intensity distribution in an absolute scale and its model fit taking into account the effect of resolution function. The dash line represents the theory and the solid line the theory convoluted with the resolution function. It illustrates the importance of fitting the data with the resolution effect taken into account properly. The lower panel gives the normalized intraparticle structure factor $\overline{P}(k)$ (dotted line) and the interparticle structure factor $S(k)$ (solid line) for a 44.0 wt % Pluronic $L64$ solution in D_2O at 53 °C. The interparticle structure factor is calculated by solving OZ equation with the short-range attractive intermicellar potential and the intraparticle structure factor is calculated using the modified cap-and-gown model [8] as described in Secs. III A and III B. The observed SANS data is the product of these two functions and therefore it is clear that the interaction peak observed in the SANS data is primarily due to the first diffraction peak in the intermicellar structure factor.

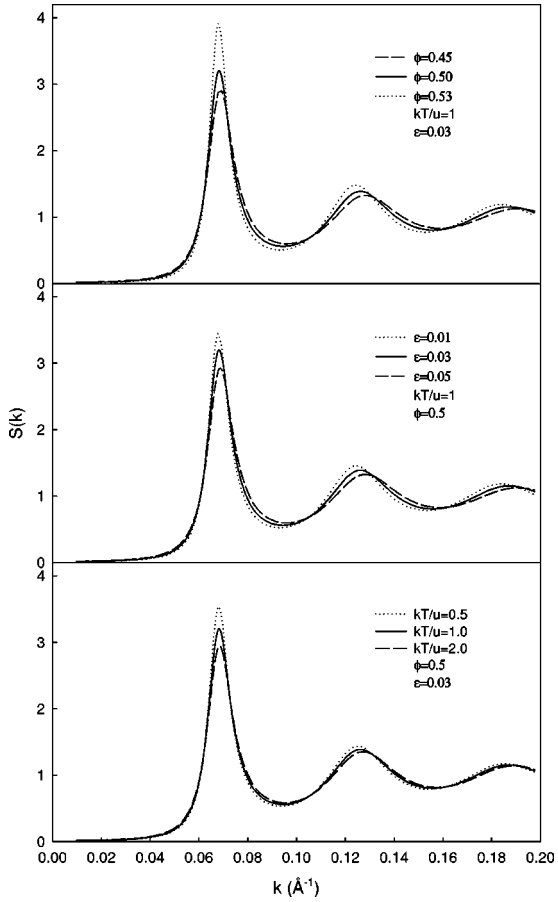

FIG. 8. The intermicellar structure factor as a function of the volume fraction, the fractional range of attractive interaction compared to the hard sphere diameter, and the depth of the potential well compared to k_BT. The top panel illustrates the sensitive dependence of the position and the height of the first diffraction peak on the volume fraction. When the volume fraction is higher, the peak is higher. The middle panel shows the height of the first diffraction peak as a function of the fractional width ε of the attractive well. When the well is narrower, the peak is higher. The lower panel gives the dependence of the height of the peak on the parameter k_BT/u $(=T^*)$. When the potential well is deeper, the peak is higher.

polymer weight fraction of 44.0 wt % at a series of temperatures ranging from 24.0 °C to 54.0 °C in Fig. 5. It can be seen that the scaled intensity distributions become temperature dependent for this concentration. We would like to mention that due to the absence of spots in the 2D ring patterns of the SANS intensity distributions, the states of the system can be identified as being amorphous but with two different degrees of disorder, depending on the temperature. One is similar to that shown in Fig. 4 and the other is much sharper and resolution limited. At this concentration a reentrant phenomenon can be seen from the inset where there are sudden sharp breaks in dimensionless line width from 0.24 to 0.1, occuring when the temperature increases from 30.0 °C to 31.0 °C and comes back to 0.24 °C, when the temperature further increases to 48.0 °C. The similar reentrant phenomena are observed for the micellar solutions with concentrations ranging from 35.5 wt % to 51.0 wt %. The transition temperatures where the reentrances occur are consistent with the transition temperatures observed by PCS and viscosity measurements, as shown in Fig. 3. The sharpness of the scaling peaks that are resolution limited indicates that the nearest neighbor distance in the glassy state (ranging from 31.0 °C to 48.0 °C) is more uniform than that in the liquid state (below 30.0 °C and above 48.0 °C).

Figure 6 is the scaling plot of a micellar solution of weight fraction 53.0 wt % at a series of temperatures ranging from 17.0 °C to 51.0 °C. Similar to Fig. 5, the system can be characterized by a temperature-dependent degree of disorder. Judging from the height, these peaks are similar to the glass peaks that we identified in Fig. 5. It is seen that both peaks are sharp. The one with sharper peak is resolution limited and is identified as ''the replusive glass,'' while the other one is nearly resolution limited and is identified as ''the attractive glass'' (see explanation given for Fig. 13).

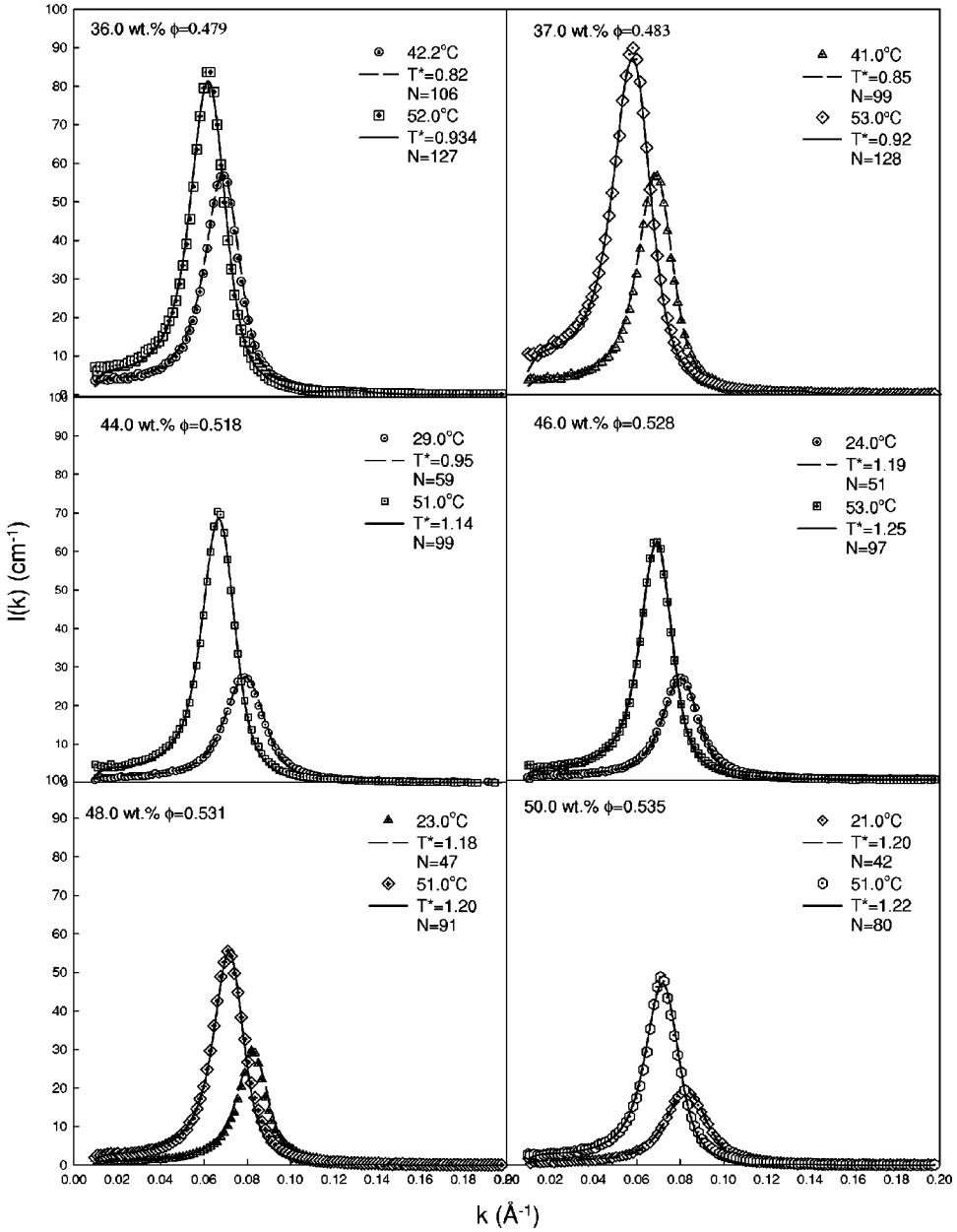

FIG. 9. Theoretical fits to SANS data taken at SAND spectrometer at IPNS, Argonne National Laboratory, for Pluronic $L64$ micellar solutions at different concentrations and temperatures. Symbols are experimental data and lines are the fits. The fits in absolute intensity scale take into account the effects of the resolution and the incoherent scattering backgrounds. The scattering intensities increase at the higher temperature liquid phase (the left-hand side peak) as compared to lower temperature liquid phase (the right-hand side peak) and the positions of the peak shifts toward smaller k due to the enhanced self-association (larger aggregation number) as a consquence of increased hydrophobicity of the polymer segments at higher temperatures.

We now start to analyze SANS intensity distributions quantatively using the model described in Sec. III. An example of SANS intensity distribution for a 44.0 wt % micellar solution at 53 °C in an absolute scale is shown together with its model fit, taking into account the effect of the resolution function in the upper panel of Fig. 7. It can be seen that the resolution correction is essential to fit the experimental data properly. The lower panel gives the normalized intraparticle structure factor $\overline{P(k)}$ (dotted line) and the interparticle structure factor $S(k)$ (solid line) for this case. The observed SANS data is propotional to the product of these two functions. The fact that the first diffraction peak of $S(k)$ occurs at relatively smooth tail part of $\overline{P(k)}$ implies that the interaction peak in the SANS intensity distribution is primarily due to the first diffraction peak in the intermicellar structure factor $S(k)$.

From Sec. III, we know that the structure factor $S(k)$ is a function of four parameters: the real particle diameter R, the volume fraction ϕ, the fractional width of the square well ε, and the effective temperature $T^*=k_BT/u$. The real particle diameter R is determined by the aggregation number N and the volume fraction ϕ (11). But the aggregation number N is

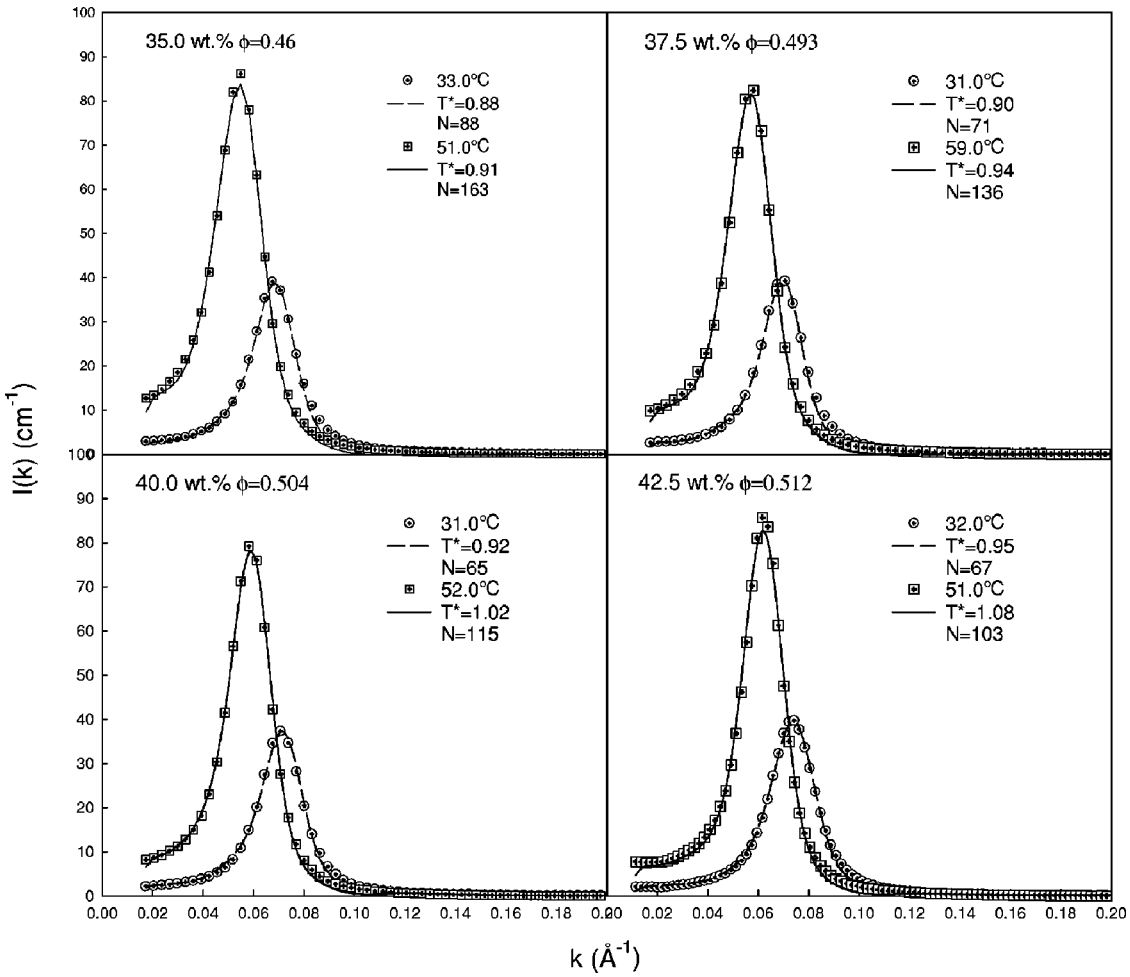

FIG. 10. Theoretical fits to SANS data taken at $NG7$ SANS spectrometer at the Center for Neutron Research, National Institute of Standard and Technology, for Pluronic $L64$ micellar solutions at various concentrations and temperatures. Although the resolution function for $NG7$ is different from the one for the SAND spectrometer at IPNS, the fits are equally good in both cases. It is important to note that from these fits we obtain unique values of four parameters: volume fraction ϕ, fractional well width ε, the effective temperature $T^* = k_B T/u$, and the aggregation number of the micelle N.

a propotionality factor to the absolute intensity (1). Therefore, for a given N, the structure factor $S(k)$ is a function of three parameters : ϕ, ε, and T^*. Figure 8 illustrates the dependence of the structure factor $S(k)$ on these three parameters. Since SANS intensity distributions reflect only intensities around the first diffraction peak, we shall comment on the behavior of this peak under the influence of each of these three parameters. It is seen from the top panel that the interaction peak is most sensitive to the volume fraction. The higher the volume fraction, the higher is the interaction peak. The middle panel shows that the higher value of ε leads to the lower height of the interaction peak. It is important to know that all the measured SANS intensity distributions (more than 150 of them) can be well fitted by a choice of $\varepsilon = 0.03$ (with an error bar of 0.01), a value consistent with our previous study of viscosity in $L64/D_2O$ system at high volume fraction [14]. The bottom panel shows that the higher the effective temperature, the lower the interaction peak.

Part of the theoretical fits to SANS data taken at SAND spectrometers at IPNS, Argonne National Laboratory, for Pluronic $L64/D_2O$ micellar solutions at different concentrations and temperatures are given in Fig. 9. Symbols are experimental data and lines are the fits. The fits in absolute intensity scale take into account the effects of the resolution and the incoherent backgrounds. It can be seen that the intensity of the higher temperature liquid phase (the left-hand side peak) and the position of the peak shift toward smaller k as temperature increases. Because of the enhanced self-association (larger aggregation number) as a consquence of the increased hydrophobicity of the polymer segments at higher temperatures, it can be seen clearly that the micelle grows when temperature increases.

Figure 10 shows the theoretical fits to SANS data taken at $NG7$ SANS spectrometer at the Center for Neutron Research, National Institute of Standard and Technology, for Pluronic $L64/D_2O$ micellar solutions at various concentrations and temperatures. Although the resolution function for $NG7$ is different from the one for the SAND spectrometer at IPNS, the fits are equally good in both cases. It is important to note that from these fits we obtain unique values of four parameters: the aggregation number of a micelle N, the volume fraction ϕ, the fractional well width parameter ε, and the effective temperature T^*.

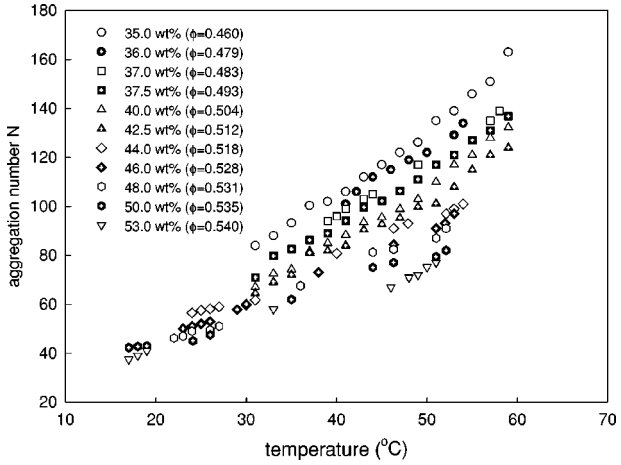

FIG. 11. Variation of the aggregation number N as a function of temperature at different concentrations. It can be seen that the degree of self-association increases as temperature increases at a given concentration. It is consistent with the fact that the PPO core becomes less hydrophilic at higher temperatures. We also note that at a given temperature, N decreases as concentration increases.

The variation of the aggregation number N as a function of temperature for different concentrations is given in Fig. 11. It can be seen that due to the fact that the PPO core in the micelle becomes less hydrophilic when heated, the micelle grows as temperature increases for a given concentration. It is to be noted that at a fixed temperature, the aggregation number decreases as a function of concentration.

Figure 12 gives the calibration curve between the ratio of the volume fraction ϕ to the weight fraction c, and c, obtained from fitting approximately 150 SANS intensity distributions. It should be noted here that the fitting results show

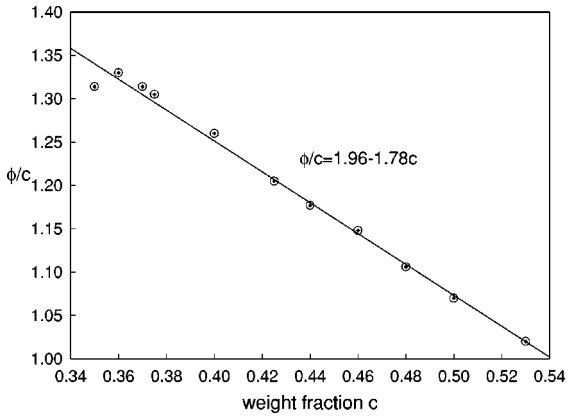

FIG. 12. The ratio of the volume fraction to weight fraction as a function of polymer weight fraction, obtained from analyses of SANS data. This is an important calibration curve that enables us to compare the experimentally determined phase diagram with the theoretical phase diagram predicted by mode coupling theory. We note that the hydration level of the micelle decreases as the polymer concentration increases. It predicts that at weight fraction 0.54 the micelle will be completely dry, since density of $L64$ is close to unity. Denoting the concentration (in weight fraction) by c and the volume fraction by ϕ, then the empirical relation is $\phi/c=1.96-1.78c$.

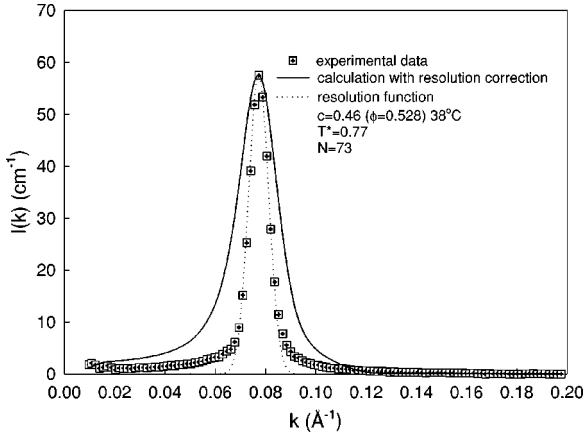

FIG. 13. The model fit of a SANS intensity distribution in the glassy state, taken with SAND spectrometer at IPNS, for Pluronic $L64$ micellar solution at 46.0 wt% and 38 °C. Symbols are the experimental data, the solid line is the theory convoluted with the resolution function, and the dotted line is the resolution function, respectively. It is clear that the experimental data is resolution limited, indicating that the system is in a nonergodic amorphous solid state. The structure factor calculated from the equilibrium liquid theory is clearly broader than the experimental data. However, the fit by the equilibrium liquid theory is sensitive to the position and the height of the interaction peak. We noted previously that the interaction peak in a SANS intensity distribution is essentially the first diffraction peak of the intermicellar structure factor $S(k)$. But the position and the height of the first diffraction peak of $S(k)$ is sensitive to the volume fraction ϕ, aggregation number of the micelle N and the effective temperature T^*. Therefore, the fitting of the position and the height of the interaction peak can still give reliable values of ϕ, N, and T^*. The fitting results shows that the depth of the intermicellar potential increases when a liquid-to-glass transition occurs upon increasing the temperature.

that the volume fraction ϕ is a unique function of concentration, independent of the temperature. The figure shows that at high concentration, the ratio of ϕ to c approaches unity, indicating that the hydration level of the micelle goes down as the concentration goes up. The mathematical relation between them is $\phi/c=1.96-1.78c$, predicting that the micelle will be dry at a weight fraction of 0.54 since the density of $L64$ is close to unity.

The SANS intensity distribution of Pluronic $L64/D_2O$ micellar solution of 46.0 wt%, at 38.0 °C (symbols) and its fitting by the theory (solid curve) are shown in Fig. 13. The fitting curve is obtained by the theory convoluted with the instrumental resolution function, which is indicated by the dotted line. It is clear that the experimental data is resolution limited. This is due to the fact that the sample is in a nonergodic state, which is an amorphous solid. Since the interaction peak of the SANS intensity distribution is essentially the first diffraction peak of the intermicellar structure factor $S(k)$, and the peak position and its height are sensitive to the volume fraction ϕ, effective temperature T^*, and aggregation number N, an accurate ϕ, T^*; and N can still be extracted from the fitting. By comparing the effective temperatures obtained from fitting the experimental data in the ergodic and nonergodic states, it can be seen that the depth of

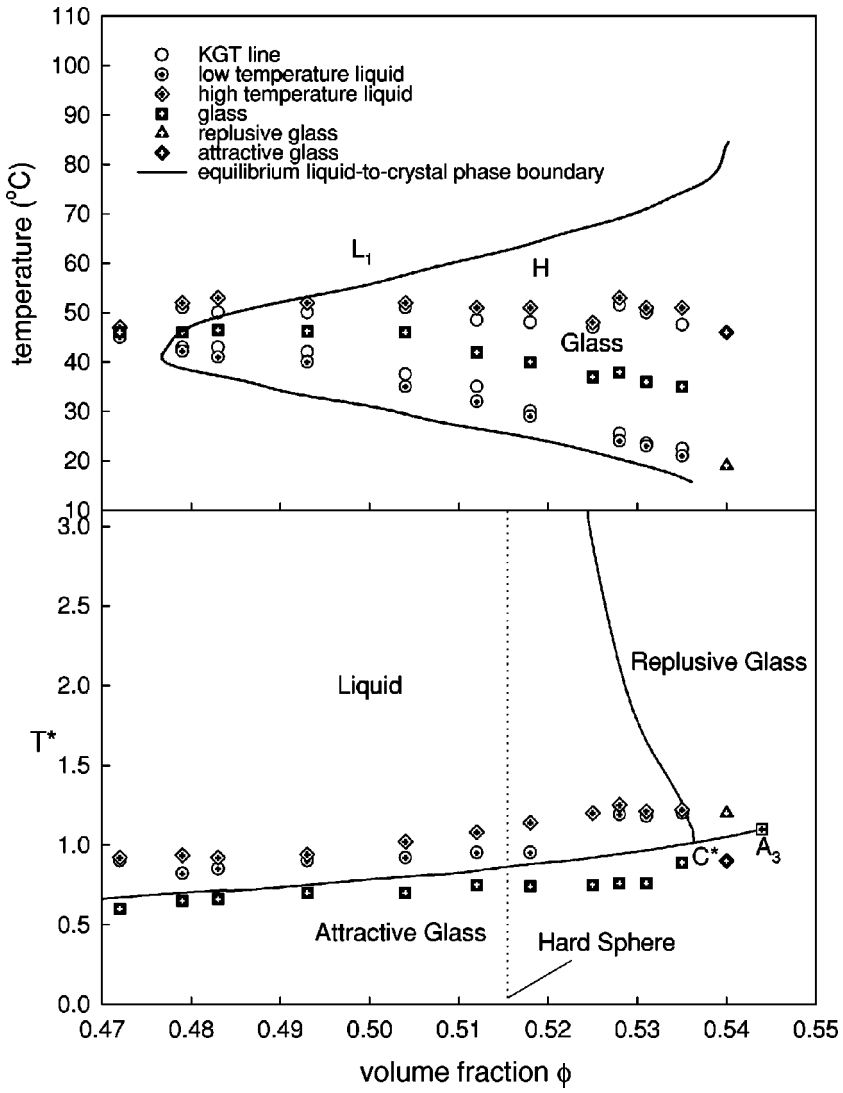

FIG. 14. Comparison of the phase diagram (in T-ϕ plane) of $L64/D_2O$ micellar solution with that of the theoretical phase diagram (in T^*-ϕ plane) determined by mode coupling theory for a colloidal system with a short-range attraction ($\varepsilon = 0.03$) [16]. In the phase diagram given on the top panel, the solid line is the equilibrium liquid-to-crystal transition line [12], empty symbols are the reentrant KGT lines, and filled symbols are the phase points where the experimental data are analyzed. The lower panel gives the theoretical phase diagram of a colloidal system interacting by a short-range attractive square well potential predicted by mode coupling theory [16]. The phase points shown in the upper panel are then mapped into the corresponding symbols in the lower panel using the results of SANS data analyses. The results of the mapping is seen to confirm the existence of the attractive branch in the predicted KGT boundary and the glass-to-glass transition (see Figs. 6 and 13).

the square well increases as the temperature increases. This make it possible for the micellar solution to transit from the ergodic liquid state to the nonergodic glass state.

Figure 14 summarizes the essential results of the extensive SANS data analysis. The upper panel gives the experimental phase diagram replotted in the temperature-volume fraction plane. It contains the equilibrium liquid-to-crystal phase boundary (solid line), the locus of experimentally determined KGT temperatures (open circles), the points of low temperature liquid locating approximately 1 °C below the lower KGT line, the points of high temperature liquid locating approximately 1 °C above the upper KGT line, and the points in glass region between the lower and upper KGT lines. The upper KGT line and the lower KGT line merge at volume fraction $\phi = 0.472$ and at a temperature of 46 °C. The lower panel shows the theoretical phase diagram predicted by mode coupling theory in the effective temperature [16] and the volume fraction plane of a colloid system with a short-range attraction, for the specific case of $\varepsilon = 0.03$ [6]. The solid line gives the liquid-to-glass phase boundaries and the symbols represent the experimental data points mapped from the upper panel. It is important to note that fitted parameters ϕ and T^* obtained by analyzing SANS intensity distributions enable us to perform this mapping and thus confirm the existence of the liquid-to-attractive-glass KGT line and the glass-to-glass transition.

V. CONCLUSIONS

Our three sets of independent experimental data clearly establish the phase boundaries of a reentrant KGT in $L64/D_2O$ micellar system. Furthermore, we use this reentrant liquid-to-glass-to-liquid transitions to substantiate the existence of an attractive branch of liquid-to-glass transition in a colloid system with a short-range attractive interparticle interaction predicted by the mode coupling calculation [3,6]. We give an evidence of the glass-to-glass transition for a sample with volume fraction of 0.54 (see Fig. 6), as predicted by the same mode coupling calculations (see the lower panel of Fig. 14).

As far as we know, this is the first time that SANS intensity distributions for a micellar solution at volume fractions larger than 0.5 have been successfully analyzed with the liquid state theory. It is our observation through analysis of more than 150 SANS intensity distributions that an attractive square well potential is necessary to fit all the data. A simple hard sphere potential will never be able to fit these data in a satisfactory way.

In a recent publication, Foffi *et al.* [17] show a phase diagram at high volume fraction for a colloid system having a short-range attractive interparticle interaction, for the case $\varepsilon = 0.03$. In this phase diagram, the KGT line lies in a metastable region sandwiched between two equilibrium liquid-to-crystal and crystal-to-crystal transition lines. This situation is similar to our observation (see Fig. 3) that the KGT lines in $L64/D_2O$ micellar system lie between a region in the equilibrium phase diagram where the hexgonal liquid crystal phase (denoted by H) and the lamellar liquid crystal phase (denoted by D) reported by Zhang, Lindman, and Coppola [12]. It is our intention to extend our SANS investigation into the concentration range between $c = 0.54$ and $c = 0.7$ in the future.

ACKNOWLEDGMENTS

The research at MIT was supported by a grant from the Materials Science Division of U.S. DOE. The research in Messina was supported by INFM-PRA98 and MURST-PRIN2000. We are indebted to Dr. Ciya Liao for taking and analyzing portion of SANS data and Dr. Emiliano Fratini for purifying $L64$ samples. We also wish to acknowledge stimulating discussions with Professor Piero Tartaglia and Professor Wolfgang Götze. Finally, we are grateful to Dr. Charles Glinka and Dr. Derek Ho of CNR (NIST), and Dr. Papanan Thiyagarajan of IPNS (ANL) for the beam time of $NG7$ and SAND spectrometers, respectively, and for their technical assistance.

[1] F. Mallamace, P. Gambadauro, N. Micali, P. Tartaglia, C. Liao, and S.H. Chen, Phys. Rev. Lett. **84**, 5431 (2000).
[2] L. Lobry, N. Micali, F. Mallamace, C. Liao, and S.H. Chen, Phys. Rev. E **60**, 7076 (1999).
[3] L. Fabbian, W. Götze, F. Sciortino, P. Tartaglia, and F. Thiery, Phys. Rev. E **59**, R1347 (1999).
[4] L. Sjögren, J. Phys.: Condens. Matter **3**, 5023 (1991).
[5] W. Götze, in *Liquids, Freezing and the Glass Transition*, edited by J.P. Hansen, D. Levesque, and J. Zinn-Justin (North-Holland, Amsterdam, 1991), p. 287; W. Götze, J. Phys.: Condens. Matter **11**, A1 (1999); W. Götze and L. Sjögren, Rep. Prog. Phys. **55**, 241 (1992).
[6] K. Dawson, G. Foffi, M. Fuchs, W. Götze, F. Sciortino, M. Sperl, P. Tartaglia, Th. Voigtmann, and E. Zaccarelli, Phys. Rev. E **63**, 011401 (2001).
[7] *Pluronic and Tetronic Surfactants* (BASF Corp., Parsippany, NJ, 1989).
[8] C. Liao, S.M. Choi, F. Mallamace, and S.H. Chen, J. Appl. Crystallogr. **33**, 677 (2000).
[9] S.H. Chen, C. Liao, E. Fratini, P. Baglioni, and F. Mallamace, Colloids Surf., A **95**, 183 (2001).
[10] The Peclet number is defined as $Pe = \dot{\gamma}\xi^2/2D_0$, which characterizes the amount of distortion of structures with linear dimension of ξ (D_0 is the particle short-time diffusion coefficient at low concentration where hydrodynamic effects dominate). These distortions are responsible for shear thinning in the system structures, which is expected to set in at $Pe \approx 1$.
[11] F. Mallamace, P. Gambadauro, N. Micali, P. Tartaglia, C. Liao, and S.H. Chen (unpublished).
[12] K.Z. Zhang, B. Lindman, and L. Coppola, Langmuir **11**, 538 (1995).
[13] S.-M. Choi (private communication).
[14] Y.C. Liu, S.H. Chen, and J.S. Huang, Phys. Rev. E **54**, 1698 (1996). Note one of the equation $\mu = \lambda\phi(1-\phi)$ was written wrongly in this paper as $\mu = \lambda\phi/(1-\phi)$.
[15] G. Foffi *et al.*, J. Stat. Phys. **100**, 363 (2000).
[16] E. Zaccarelli *et al.*, Phys. Rev. E **63**, 031501 (2001).
[17] G. Foffi *et al.*, Phys. Rev. E **65**, 031407 (2002).